공학석사 학위논문

Improved Tribological Property of Thermoplastic Elastomer Nanocomposites

열가소성 엘라스토머 나노 복합재료의

우수한 마모 저항 특성

2019년 2월

서울대학교 대학원

재료공학부

전 혜 린

Improved Tribological Property of Thermoplastic Elastomer Nanocomposites

열가소성 엘라스토머 나노 복합재료의
우수한 마모 저항 특성

지도교수 유 웅 열

이 논문을 공학석사 학위논문으로 제출함

2019년 1월

서울대학교 대학원
재료공학부
전 혜 린

전혜린의 공학석사 학위논문을 인준함
2019년 1월

위 원 장 안 철 희 (인)

부위원장 유 웅 열 (인)

위 원 이 명 규 (인)

Improved Tribological Property of Thermoplastic Elastomer Nanocomposites

Advisor: Woong-Ryeol Yu

by

Jeon Hyerin

2019

Department of Materials Science and Engineering
The Graduate School
Seoul National University

Abstract

Improved Tribological Property of Thermoplastic Elastomer Nanocomposites

Jeon Hyerin
Department of Materials Science and Engineering
The Graduate School
Seoul National University

Abrasion resistance is a property that a material can resist damage from wear. Materials with good tribological performance are used in various fields such as tiers, bearing, brake pads, shoes outsole, etc., and it is necessary to develop high abrasion resistant materials for industrial use. Conventionally, carbon black has been used as an abrasion resistant reinforcing filler, and surface modification of carbon black and dispersing agent mainly have been studied. It is possible to improve the dispersibility of filler in the polymer matrix through surface treatment, however, it has limitations, so it is necessary to study on the structural aspects of the filler.

In this study, nanocomposites were prepared with high abrasion resistance filled with exfoliated graphite (EG). EG was prepared by electrochemical exfoliation of graphite, and incorporated into elastomer as a reinforcement filler. Carbon materials were compounded with thermoplastic polyester elastomer (TPE) via multi-extrusion processes. Compared to neat polymer and nanocomposites filled with carbon black (CB) and surface modified carbon black (a-CB), EG

composites exhibit an obvious superiority in tribological performance. Since EG has a two-dimensional structure with a high aspect ratio and hydrophilic groups on its surface, it is advantageous to improve the interfacial affinity between filler and matrix rather than carbon black.

Keywords: Exfoliated graphite, Carbon black, Thermoplastic elastomer, carbon nanocomposites, Improved tribological properties

Student Number: 2017-24895

Contents

List of Figures

1. Introduction

1.1. Tribology

1.1.1 Introduction

Friction and wear is a very common phenomenon in everyday life and industry that depend on the process, which occurs in a thin layer of the object in moving contact [1]. Wear is the gradual removal of material at solid surfaces by damage, or deformation. Wear of materials can be result from mechanical or chemical causes, such as erosion or corrosion. Wear of the machine element, fatigue or creep, will degrade the functional surface and eventually result in performance degradation or loss. Therefore, the effect of friction and wear on energy consumption, carbon emissions and economic expenditures is considerable. Thus the review on wear and related processes of materials, which called 'tribology' has been studied, since the mid-20th century [2].

1.1.2 Types of wear

Wear types are commonly classified by its mechanism: abrasive wear, adhesive wear, and surface fatigue [3]. First, abrasive wear is generally defined as material removal at the hard surface due to sliding contact with a rough surface or abrasive particles [4]. In other words, abrasive wear occurs when hard and sharp surface glides over a soft surface, digging out a groove. This means that the sliding materials have different relative hardness [5]. It is the most important type of wear because it accounts for almost 63% of the total wear cost [6]. Traditionally,

abrasive wear is divided into two-body (Figure 1. (a)) and three-body abrasive wear (Figure 1. (b)) [7]. Two-body abrasive wear occurs when hard protrusions on one side slip on the other, while three-body abrasive wear occurs when rigid particles are stuck between two solid surfaces [8]. The rigid particle is the third component, such as sand grains in a bearing abrasive material [5]. In most cases where two- or three-body abrasive wear occurs, abrasion occurs on a softer surface regardless of wear rate [4].

Second, adhesive wear is due to the adhesive bond on the contact faces between two sliding materials, which called the junction. If one of the junctions does not recover along the original surface, the wear debris from one of the two contact faces is transferred to the other surface. In other words, adhesive wear occurs when the atomic force between the two sliding materials is stronger than the unique material properties of each surface. For instance, when the contact surfaces are sliding, the bonding of protrusions occurs. Then, the wear particle from weaker substances are produced, because continuous movement of the surface will break the bond junctions (Figure 1. (c)) [5].

Finally, surface fatigue wear occurs as a result of crack formation and growth. It takes place when the strains or cyclic shear stresses in softer surface exceeds the fatigue limit of the material. The damage of fatigue wear ranges from a very small area to a large area, which have microscopic diameters or macroscopic diameters. It is the main cause of wear of rolling devices such as ball bearings, wheels on gears and rails. Cracks form on the surface and gradually grow until the large wear debris broke off the surface (Figure 1. (d)) [5].

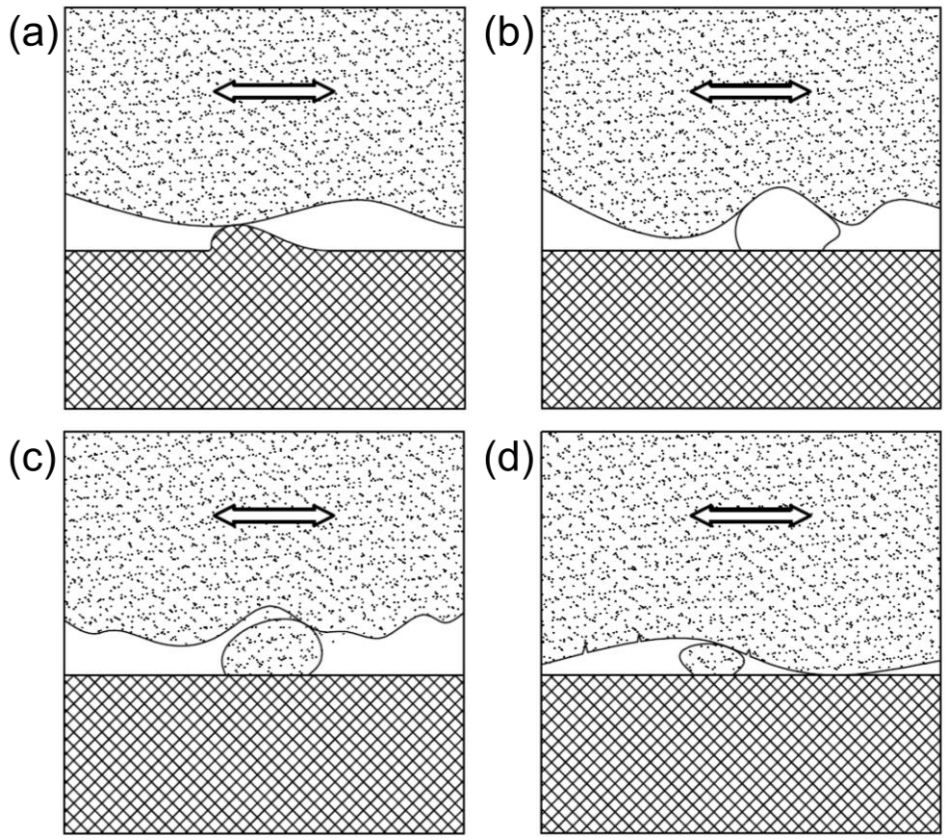

Figure 1. Wear types according to wear mechanism: (a) two-body abrasive wear, (b) three-body abrasive wear, (c) adhesive wear, and (d) surface fatigue wear [5].

1.1.3 Wear in polymer

Polymers have been widely used in most industries due to their excellent physical, chemical properties, good processability, and cost effectiveness. When polymers are used on the wear or friction surface, such as bearings, gears, guides, seals and artificial joints, the tribological properties of the polymer play a key role. In recent years, there has been a steady interest in research to improve the chemical, physical properties and wear resistance of polymers. By enhancing or modifying the polymer, their application can be extended to a wider industrial scope [9].

Recently, many laboratories are conducting research on composite materials containing nanometer-sized particles. For instance, when the inorganic particles of nano size is added to the polymer, it is possible to improve the toughness of the material and frictional performance [10]. If the nano-filler is uniformly dispersed in the polymer matrix, it can cause strong interfacial interactions in a significant portion of the exposed atoms at interfaces, due to the ultrafine dimensions of the nanoparticles. As a result, nanocomposites combined with numerous interfaces are expected to have outstanding performances [11].

Therefore, nanostructured materials have attracted attention because they have a wide range of potential applications in many fields. For example, multi-walled carbon nanotube (MWCNT) is the one of fillers used for nanocomposites, and they has been widely used in the fields, such as micro-contact printing, artificial muscles, microwave absorption devices, nano-fluidic devices, and functional carbon nanotube devices [12-16].

In recent years, several studies on the improved properties of polymer nanocomposites have been carried out, some of them was a study of the elastomer nanocomposites. In this study, the nanocomposites with improved abrasion resistance were fabricated using nanoscaled carbon filler and elastomer [17].

1.2. Carbon black

1.2.1 Introduction

Carbon black refers to almost amorphous or paracrystralline carbon particles with small size, grown to form aggregates. Carbon black is manufactured in the gas phase by the incomplete combustion or thermal decomposition of hydrocarbons. Commercial carbon black is classified into various grades depending on the size and shape of its particle and aggregates, surface area, porosity and surface properties [18].

Carbon black is composed of spherical primary particles whose diameter is ranging from tens to hundreds of nanometers, and they fused to form a larger units, called 'aggregates'. The aggregates are linked together with weak bonds in order to form a high order branched structure, which called 'agglomerates' (Figure 2). Their shape and size are depending on primary particle of the carbon black, the nature of the matrix and the mixing process conditions (Figure 3) [19-21].

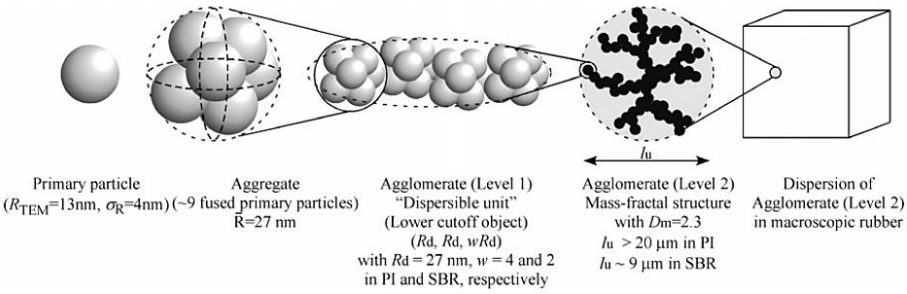

Figure 2. Schematic illustration for the hierarchical structure of the carbon black in a rubber matrix [21].

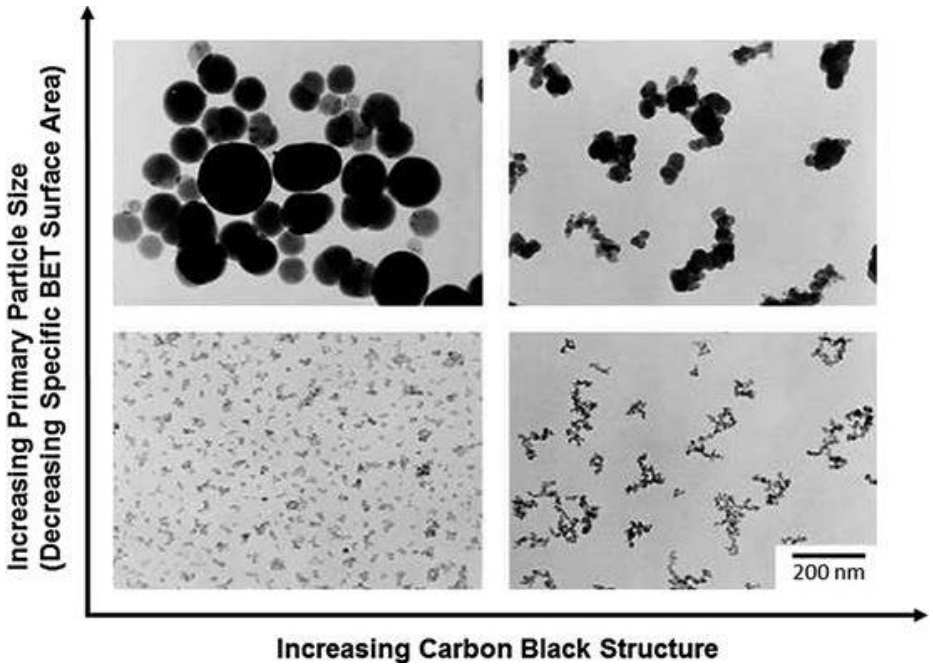

Figure 3. TEM image of agglomerates with different shape, according to the size of primary particle and structural complexity [18].

1.2.2 Applications

If carbon black is added as a filler in a polymer matrix, it improves the mechanical properties of the polymer and makes the polymer, an insulator, conductive in order to manufacture the antistatic polymer. Specialty grades of carbon black are used as black pigments in inks, paints, and plastics. In addition to, they are used as ultraviolet (UV) stabilizers for polymers to prevent their degradation from visible and UV light [18].

However, the largest application of carbon black is a reinforcing filler for elastomer, such as rubber products like tires. The reinforcing effect of the carbon black composite material is influenced by interfacial affinity between the carbon black - carbon black particles, the polymer - polymer molecules, and the carbon black - polymer molecule. The interfacial affinities between them are highly dependent on the morphology and microstructure of carbon black, such as the size, structure, surface area and surface properties. Particularly, resulting from these characteristics, dispersibility of the carbon black in the polymer matrix is the most important factor for outstanding properties of the composite material [18,22,23].

1.3. Exfoliated graphite

1.3.1 Introduction

Graphene is a single layer of carbon atoms forming a honeycomb arrangement of sp^2 bonds, which is an allotropes of carbon, such as graphite, carbon nanotube, charcoal, diamond and fullerene. Graphene was expected to be capable of production in theory from 1947. However, there was no technology to separate graphene from bulk graphite. In 2004, Geim and Novoselov succeeded in isolating graphene for the first time, using scotch tape. Graphene shows exceptional mechanical, electronic, and thermal properties [24,25]. The monolayer graphene has high intrinsic strength of ~130 GPa and Young's modulus of 0.5-1.0 TPa [26]. Also, it can bear several million times the maximum current density that copper can withstand [27]. Moreover, monolayer graphene has a high thermal conductivity of 1500-2500 $Wm^{-1}K^{-1}$ [26-28]. Due to these excellent properties, there have been attempts to apply graphene to various fields, such as advanced composites, electronic devices, sensors, batteries and supercapacitors [27,29,30]. Therefore, interest in the scalable production of graphene has been steadily increasing, because of its unique properties and promising applications [31].

A number of methods for producing graphene have been proposed and studied, so far. These methods can be classified into two main classes: bottom-up and top-down methods. The bottom-up methods, such as chemical vapor deposition (CVD) use a chemical reaction to create a planar carbon structure covalently bonded. CVD can be used to produce high-quality graphene with large-area and low-defect, suitable for electronic devices. However, the method is inappropriate for the mass production of graphene due to several obstacles, such as multi-step process for transfer onto desired substrates, high reaction temperature, expensive equipment, and limited production [32-34].

Larger amount of graphene can be manufactured by top-down methods, like Hummers' method and other exfoliation methods. Using top-down methods, it has been demonstrated that graphene mass production is possible at a low cost [35,36]. Chemical exfoliation of graphite based on the Hummers' method is an attractive method in terms of mass production, but it produces graphene oxide (GO) with defects and oxygen functional groups on the surfaces. Therefore, in order to recover the electronic properties of the graphene sheet, chemical or thermal reduction must be performed. After the reduction process, reduced graphene oxide (r-GO) is produced, which restore only a part of the characteristics of graphene. Several direct exfoliation methods have been proposed to overcome the limitations, such as thermal, mechanical and electrochemical exfoliation [37]. Using these exfoliation methods, adjacent carbon layers are separated, but typically separation doesn't occur at all layers. Thus, as a result of exfoliation, a multilayer graphene material is obtained, which is called exfoliated graphite (EG) [38].

1.3.2 Mechanical exfoliation of graphite

To peel graphene sheet from bulk graphite, the van der Waals attraction between adjacent graphite layers must be overcome. Attraction force between the carbon layers can be solved by mechanically exfoliation methods. Generally, there are two routes of separating EG from bulk graphite mechanically: normal force and lateral force. The normal force is the force applied vertically to overcome the van der Waals attraction between the carbon layers (Figure 4. (a)), and this route is applied to the scotch tape method [25,39]. The shear force can be promoted by self-lubricating ability of graphite layer in lateral direction (Figure 4. (b)). All of the mechanical exfoliation methods reported so far are based on these two pathways, therefore by adjusting the two routes, it will be able to control the exfoliation process and the production of the high-quality graphene [31].

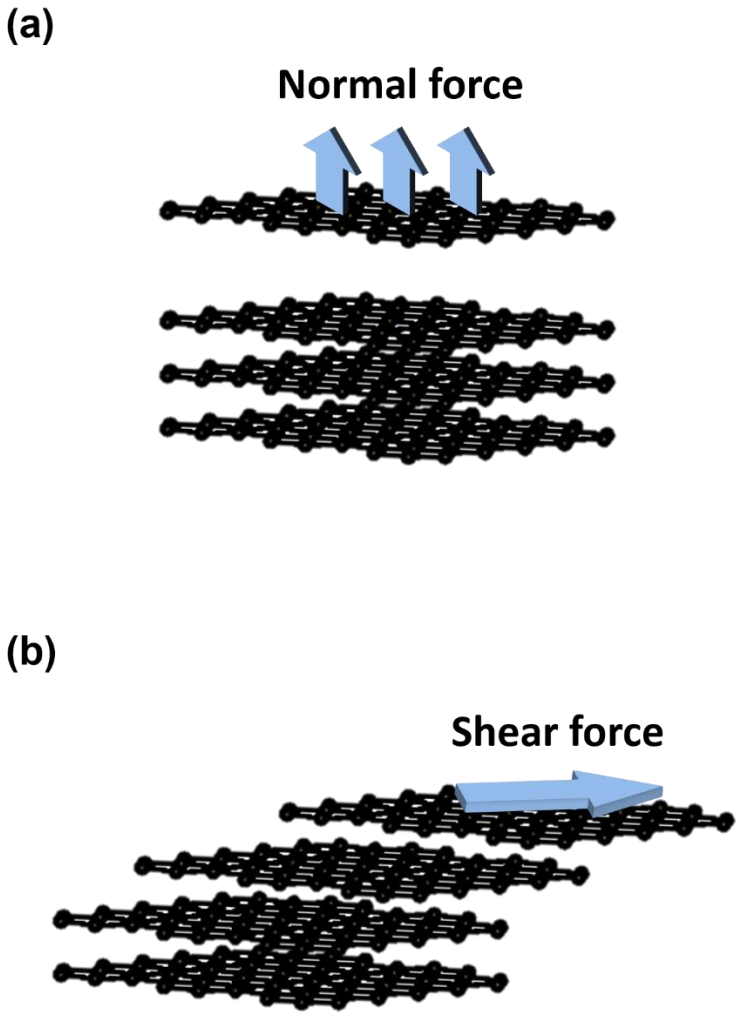

Figure 4. Two routes for mechanical exfoliation of graphite: (a) normal force, and (b) shear force.

1.3.3 Electrochemical exfoliation of graphite

In recent years, electrochemical exfoliation of graphite has attracted interest in graphene production, because it is easy, fast, scalable, and environmentally friendly [40-42]. The electrochemical method make graphite intercalation compounds (GICs), by intercalating molecules between the graphite layers using the graphite as an electrode with its electrical conductivity. A positive or negative charge is applied to the graphite electrode, in order to facilitate the intercalation of the counter-charged ions and exfoliation (Figure 5). Preparation of EG by electrochemical method does not require the use of harsh chemicals, which can lead to simpler product purification steps. Since the oxidation level can be controlled by the electrochemical method, the obtained EG is comparatively high-quality with less defects. In addition to, functionalized graphene can be manufactured in a one-pot process using the electrochemical method [43].

Generally, the process is carried out using an aqueous acid solution or ionic liquid as the electrolyte. Exfoliation in aqueous acid solution can produce relatively high-quality EG with large lateral size, and significant amount of oxygen functional groups due to the peroxidation by acid electrolyte [40,44]. On the other hand, when exfoliation is carried out in ionic liquids, EG is produced in relatively small amounts, and tends to have a small lateral size (<5 μm). Therefore, it is necessary to use an appropriate electrolyte system that takes into account both aspects of high-quality EG production or mass production [24].

In this study, surface treated carbon black (a-CB) and electrochemically exfoliated graphite (EG) were prepared as fillers for elastomer. The carbon fillers were added and compounded to thermoplastic polyester elastomer (TPE) via multi-extrusion processes. Wear test specimens of nanocomposites using these carbon fillers were prepared and the tribological properties of each material were evaluated.

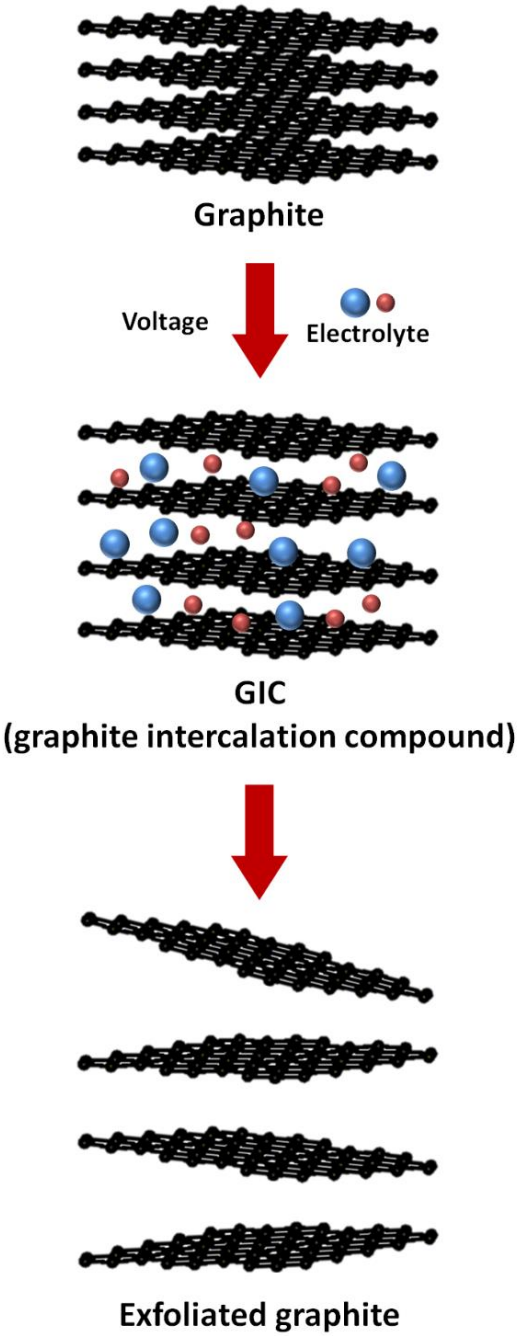

Figure 5. Schematic illustration of electrochemical exfoliation of graphite.

2. Experimental

2.1. Materials

Carbon black (CB, N330) which manufactured for high abrasion resistance uses with particle size of 30-50 nm, was obtained from OCI. A graphite foil with thickness of 0.5 mm, was purchased from Alfa Aesar. The reagents and solvents were purchased from Samchun, nitric acid (HNO_3) and ammonium sulfate ($(NH_4)_2SO_4$), and used without further purification. Thermoplastic elastomer (TPE), especially which has polyester moiety, TRIEL was purchased from Samyang with melt flow index of 11 g/10 min and melting point of 210ºC.

2.2. Fabrication of carbon fillers

2.2.1 Surface modification of carbon black

A 1,000 mL two-neck flask connected to a condenser was charged with 10 wt. % nitric acid aqueous solution (500 ml), carbon black (5 g) and a stir bar. Surface modification of carbon black was carried out at 150ºC, for 24 hours with stirring. After the treatment, carbon black was thoroughly washed with deionized water until pH 7. The product was dried in vacuum oven at 120ºC, over 24 hours for fabricating nanocomposites.

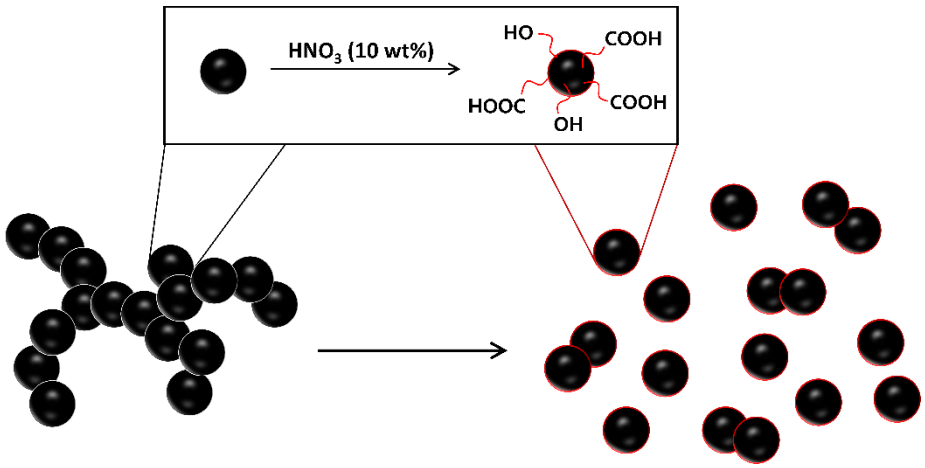

Figure 6. Schematic illustration of surface modification process.

2.2.2 Electrochemical exfoliation of graphite

A graphite foil (35 mm × 75 mm × 0.5 mm) was used as a working electrode (i.e., anode) for electrochemical exfoliation. A stainless-steel electrode was used as a counter electrode (i.e., cathode). Both electrodes were placed parallel, in 0.5 M ammonium sulfate aqueous solution, the electrolyte for electrochemical exfoliation. The distance between the two electrodes was kept constant at 2 cm throughout the exfoliation process.

A positive voltage (+10 V) was applied to the EG electrode, at room temperature. After the exfoliation, the product thoroughly washed using deionized water by vacuum filtration, in order to remove the residual salts. The electrochemically exfoliated graphite (EG) was obtained by vacuum dry at 120ºC, over 24 hours.

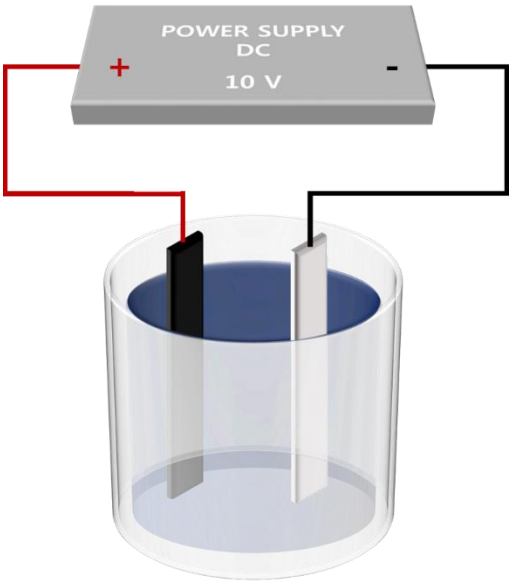

Figure 7. Schematic illustration of electrochemical exfoliation of the graphite foil.

2.3. Preparation of carbon/TPE nanocomposites

The nanocomposites with 1 phr carbon filler were prepared by a melt-compounding method. TPE was dried in vacuum oven at 70ºC, over 24 hours, before the process in order to avoid moisture-induced degradation. The melt-compounding was carried out using a single screw extruder (3D factory, Korea, ϕ=20 mm, L/D=27) and a twin screw extruder (BA-19, Bautek, ϕ=19 mm, L/D=40).

At first, each carbon filler such as carbon black (CB), surface modified carbon black (a-CB), and electrochemically exfoliated graphite (EG) was premixed with TPE, using the single screw extruder. The temperature profile of the extruder from Zone 1 to Zone 4 was set to be 80, 220, 250 and 240 ºC. The screw speed was fixed at 150 rpm. Then, the product was compounded through a twin screw extruder to evenly disperse the carbon filler in the polymer matrix. The temperature profile of the extruder from Zone 1 to Zone 6 was set to be 120, 235, 245, 250, 245 and 240 ºC. The screw speed was fixed at 110 rpm. The extruded strands (average diameter = 1.75 mm) were cooled into water bath, and used for 3D printing application or pelletized for fabricating specimens. The nanocomposite specimen of disc shape with diameter of 100 mm for abrasion tests, were prepared by the compression-molding method.

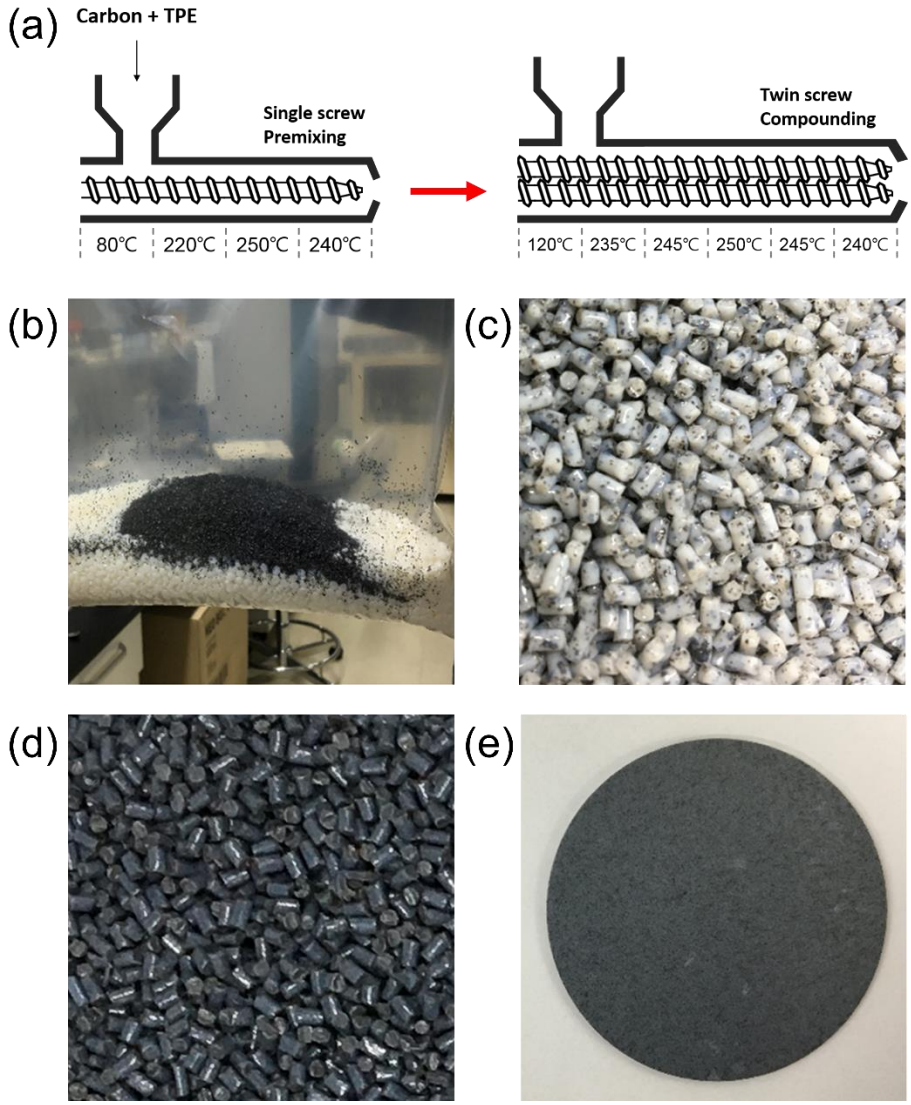

Figure 8. Preparation of nanocomposite: (a) premixing and compounding via multi-extrusion process, (b) EG and TPE, (c) product after premixing by single screw extruder, (d) product after compounding by twin screw extruder, and (e) nanocomposite specimen for the wear test.

2.4. Characterization of carbon fillers and nanocomposites

The functional groups of carbon fillers were investigated by Diffuse Reflectance Infrared Transform (DRIFT, Nicolet 6700, Thermo Fisher Scientific Inc.), in the range of 500-4000 cm^{-1}. The C/O ratio and the content of functional groups containing oxygen of carbon fillers were evaluated by X-ray photoelectron spectroscopy (XPS, KRATOS, AXIS Nova) using monochromatic Al Kα radiation. Carbon fillers were investigated by Raman spectrometer (BRUKER, SENTERRA). The thickness and shape of EG was taken from atomic force microscopy (AFM, BRUKER, Nanoscope). Surface morphology of carbon fillers and nanocomposites were investigated using scanning electron microscope (SEM, COXEM, CX-200TA), and field emission SEM (FE-SEM, Tescan Mira 3 LMU FEG). The tribological tests of the nanocomposites were carried out using a universal ring-plate abrasion tester (Taber, Model 5132) following ASTM D4060, two abrasive wheel (CS-17) were used as the counterparts. The nanocomposites specimen were fastened on the tester, as the countertops. All experiments were conducted under the conditions (room temperature, humidity: 8−15%, total cycle: 1000 r, rotational speed: 60r/min, normal load of 1000 g). The specimens were weighted using an analytic balance, before and after the tests. Then, the wear loss of the nanocomposites was evaluated by calculating the weight difference before and after the test. The 3-dimensional profiles of nanocomposites' worn surface were taken using Alpha step (BURUKER, DektakXT Stylus Profiler), and also, the surface roughness of specimen also obtained from the Alpha step.

3. Results and Discussion

3.1. Characterization of carbon fillers

3.1.1 Morphology investigation

3.1.1.1 SEM

Morphology features of carbon black (CB), surface modified carbon black (a-CB) and electrochemically exfoliated graphite (EG) were characterized by scanning electron microscope (SEM), as shown in Figure 9. Pristine carbon black has a branched structure composed of spherical particles, and each particle size is about 30-50 nm (Figure 9. (a)). a-CB shows a slightly smoothed surface without significant damage to the particles despite the acid treatment (inset of Figure 9. (a), (b)). On the other hand, the electrochemically exfoliated graphite has a two-dimensional crumpled sheet structure, and its lateral size is about 2-50 μm (Figure 9. (c)).

3.1.1.2 AFM

The thickness and roughness of EG sheets was investigated by AFM. Several EG sheets were selected randomly, and two of them were shown (Figure 10). AFM images show that the EG exhibits crumpled sheet structure and the thickness of EG was evaluated in the range of 4.2-9.5 nm. It can be seen that the EG was prepared in the form of a multi-layer graphene comprise of 6 to 14 fundamental layers by electrochemical exfoliation (monolayer graphene = 0.65 nm).

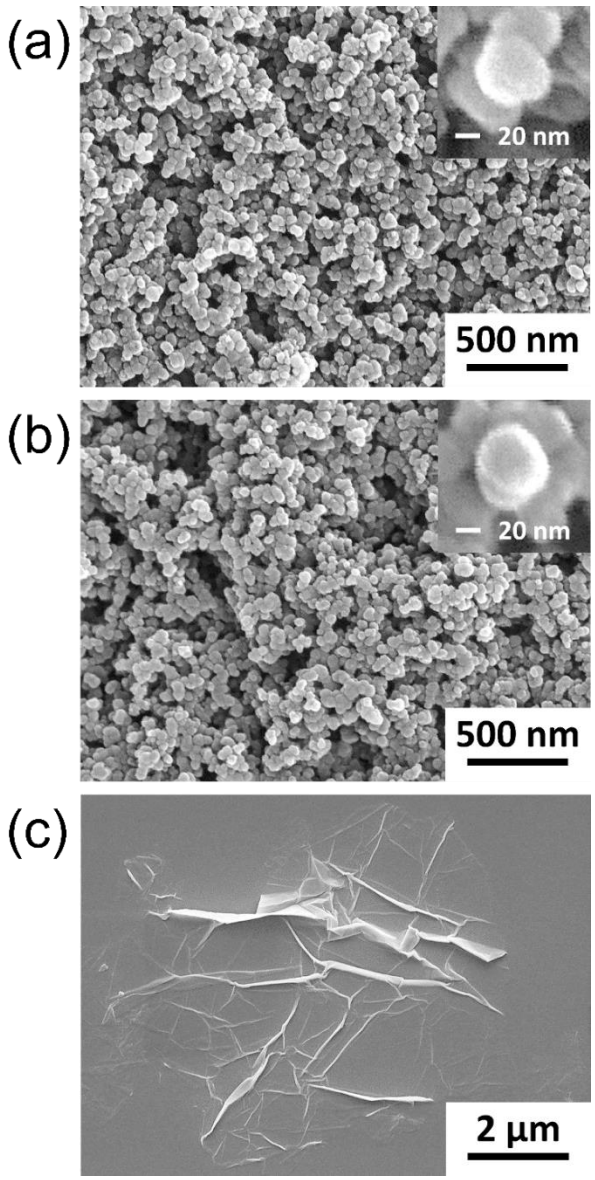

Figure 9. SEM image of carbon fillers: (a) CB, (b) a-CB, and (c) EG.

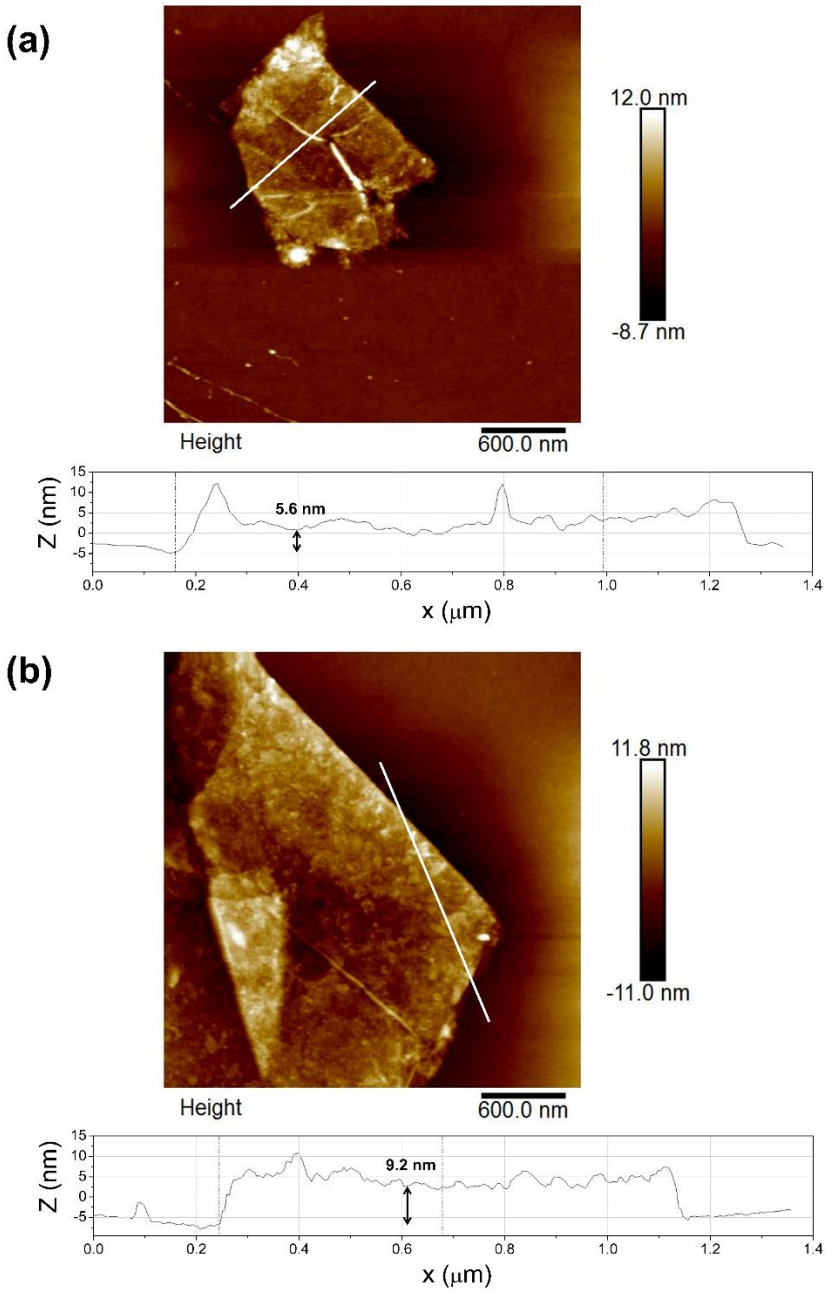

Figure 10. AFM image EG sheets prepared by electrochemical exfoliation, in the form of a multi-layer graphene.

3.1.2 Characterization of chemical structure

3.1.2.1 Diffuse Reflectance Infrared Fourier Transform (DRIFT)

The chemical structure of CB, a-CB and EG is identified by DRIFT (Figure 11). All three samples exhibited a strong band at around 3440 cm^{-1} and 1630 cm^{-1} (O–H stretching, and C=C stretching, respectively). Except for two bands above, the CB shows spectra with almost no characteristics, whereas new bands were observed at 1670 cm^{-1}, 1479 cm^{-1} and 1269 cm^{-1} (C=O stretching in carboxyl acid group, O-H bending vibration and C–O stretching vibration, respectively) in spectra of a-CB. It can be deduced that a hydrophilic group such as –COOH or –OH is formed on the surface of the carbon black by treating with nitric acid. These hydrophilic groups cause electric repulsion and steric hindrance which are advantageous for dispersing large agglomerates into small particles in polar medium [45]. Therefore, it can be expected to a-CB has better dispersibility in the polar polymer matrix, than CB due to the functional groups, including oxygen, introduced on the a-CB surface.

Meanwhile, EG showed bands at 1713 cm^{-1} (C=O stretching in carboxyl acid) as well as 1265 cm^{-1} (C–O stretching vibration) similar to a-CB. Furthermore, EG showed a new band, not found in CB and a-CB, at 1041 cm^{-1} (C-O of phenolic hydroxyl groups), thus it can be inferred that EG has a graphitic planar structure in which the aromatic rings incorporating hydrophilic groups are continuously connected.

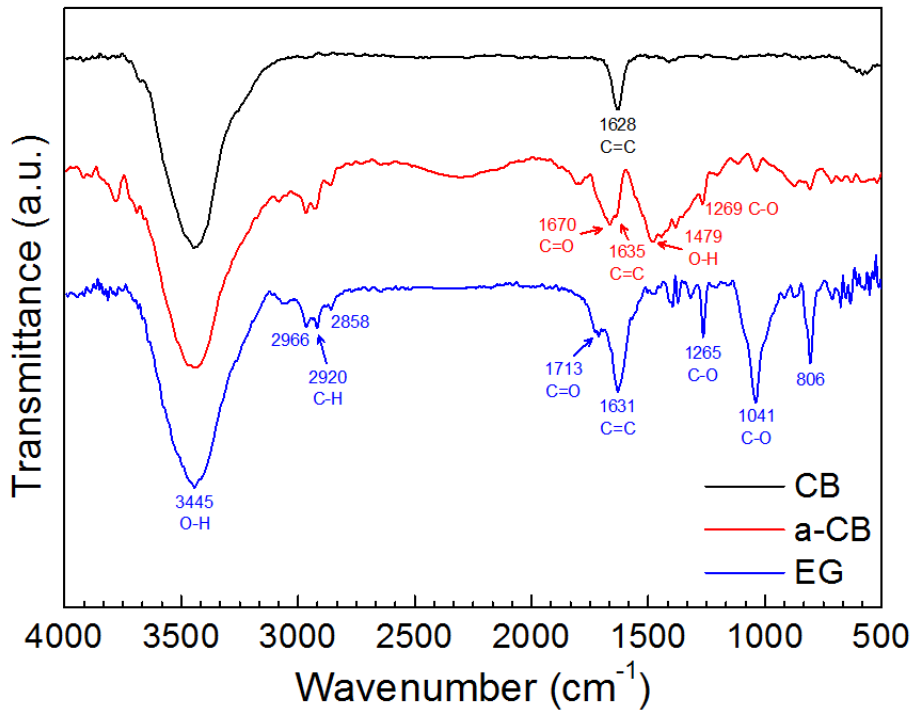

Figure 11. DRIFT spectra of carbon fillers: CB, a-CB, EG.

3.1.2.2 Raman

The carbon fillers were also analyzed by Raman spectroscopy to probe the carbon structure (Figure 12). Raman spectra of carbon material has two characteristic peaks: the D (disorder or defect) peak and G (graphite) peak, which designates sp^3 hybridized carbon and sp^2 hybridized carbon, respectively. In general, the G peak and the D peak appear approximately 1580 cm^{-1} and 1350 cm^{-1}, also the intensity ratio of these two peaks, I_D/I_G, can be used to evaluate the microstructure of the material [46]. The spectra of CB and a-CB similarly exhibit a D peak near 1380 cm^{-1} and a G peak near 1590 cm^{-1}. In both spectra, the D peak and the G peak are broadly formed and overlapped, so they are not clearly separated, which is a feature that is commonly found in amorphous carbon. The I_D/I_G of the CB was 1.0 and that of the a-CB was 1.1, which suggests that functional groups were introduced on the surface of carbon black and its structural order was slightly reduced through the acid treatment [47]. Unlike the above two samples, in a spectrum of EG the G peak was clearly separated at 1355 cm^{-1} from the D peak at 1583 cm^{-1}, and its I_D/I_G was 0.24, indicating EG has highly ordered structure than CB and a-CB. In addition, EG shows a 2D peak which was not found in CB and a-CB, near 2710 cm^{-1}, which is a peak appearing in multi-layered materials such as graphene, due to the various scattering processes caused by the number of energy bands. In previous studies, Li, X. et al. reported that the number of layer of graphene can be measured by the I_{2D}/I_G, as the intensity ratio to the 2D peak and G peak. Their results indicated that I_{2D}/I_G of one layer-graphene should be 1.5 or more, and that of two layer-graphene should be about 1. Lastly, the I_{2D}/I_G ratio of multi-layer-graphene which has four layers or more should be 0.6 or less [48]. Indeed, I_{2D}/I_G of EG was 0.38, suggesting that the multi-layer graphene was prepared through the electrochemically exfoliating of graphite.

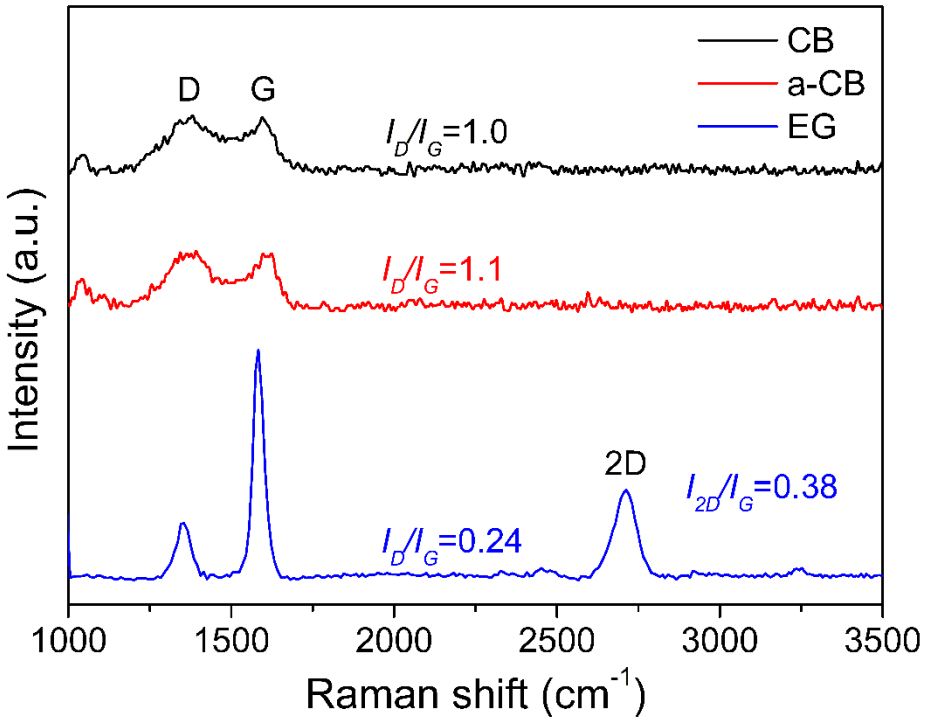

Figure 12. Raman spectra and I_D/I_G ratio of carbon fillers: CB, a-CB, EG.

3.1.2.3 X-ray photoelectron spectroscopy (XPS)

XPS analysis was carried out to investigate the chemical states of the elements on the surface of the fillers. XPS survey scan spectra of CB, a-CB and EG exhibited a strong C1s peak at 284.5 eV and O1s peak at 532.3 eV (Figure 13. (a)). Through the surface treatment of carbon black, the intensity of the C1s peak slightly decreased whereas that of the O1s peak increased. In fact, C/O ratio decreased from 34.0 (CB) to 9.98 (a-CB), indicating that the proportion of oxygen functional groups bonding with carbon element increased after functionalization. Meanwhile, C/O ratio of EG was 13.7 which is between that of CB and a-CB. Furthermore, the C1s peak of each fillers deconvoluted into the four peaks in order to determine the presence of which oxygen functional groups on surface (Figure 13. (b), (c), and (d)). The C1s peaks were disassembled into four peaks and assigned to C=C–C (284.5 eV), C–O (285.9 eV), C=O (288.0 eV), and O–C=O (289.8 eV) [49]. The C1s spectrum of a-CB showed an overlapped structure with a loose tail at higher binding energy, while the CB showed a tiny tail shape. It can be seen that, the atomic percentage of the carboxyl group (O–C=O) increased from 6.0 to 11.0, after functionalization, suggesting that acid treatment can significantly affect the chemical composition of carbon black, especially amount of carboxyl groups. These hydrophilic groups are expected to contribute to increasing the dispersibility of the filler in polymer matrix, which is consistent with the aforementioned results of DRIFT, Raman and XPS survey scans. On the other hand, EG showed a relatively sharp C=C–C bond and a weak tail at higher binding energy. It was found that the C–O functional group such as epoxide or phenolic hydroxyl group was the most abundant on the surface of EG.

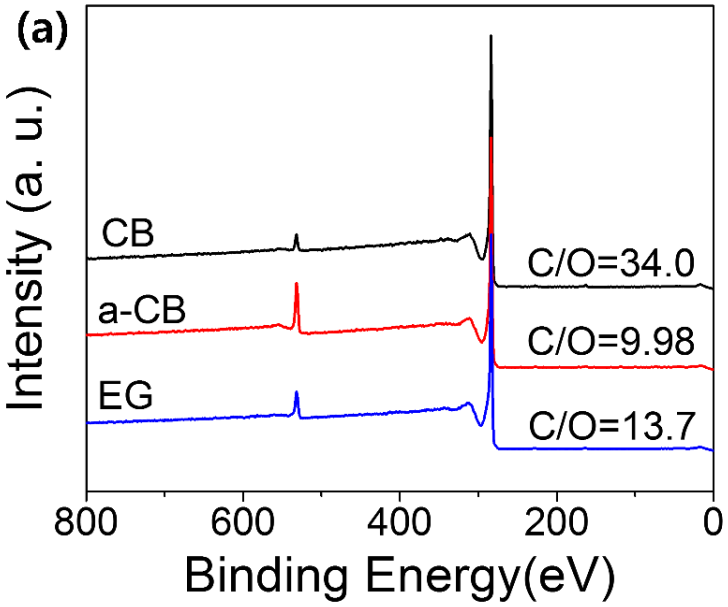
(a)
Intensity (a. u.)
CB
a-CB
EG
C/O=34.0
C/O=9.98
C/O=13.7
800
600
400
200
0
Binding Energy(eV)

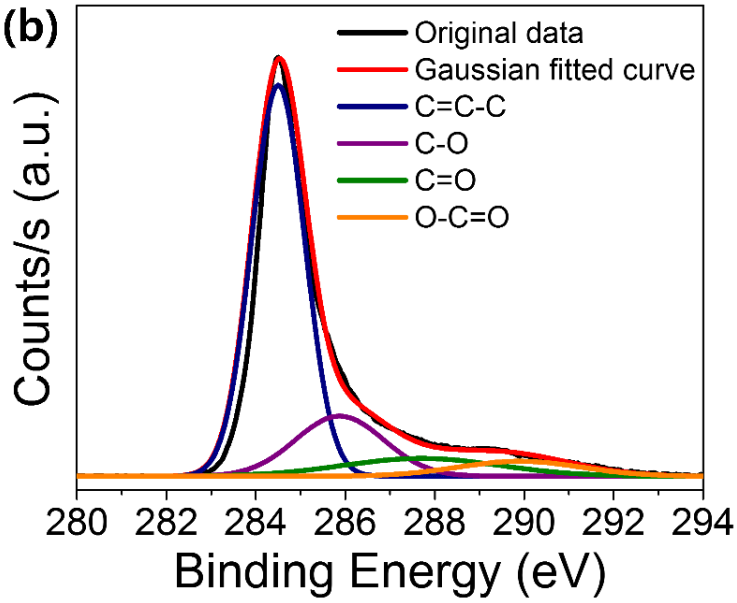
(b)
Counts/s (a.u.)
Original data
Gaussian fitted curve
C=C-C
C-O
C=O
O-C=O
280
282
284
286
288
290
292
294
Binding Energy (eV)

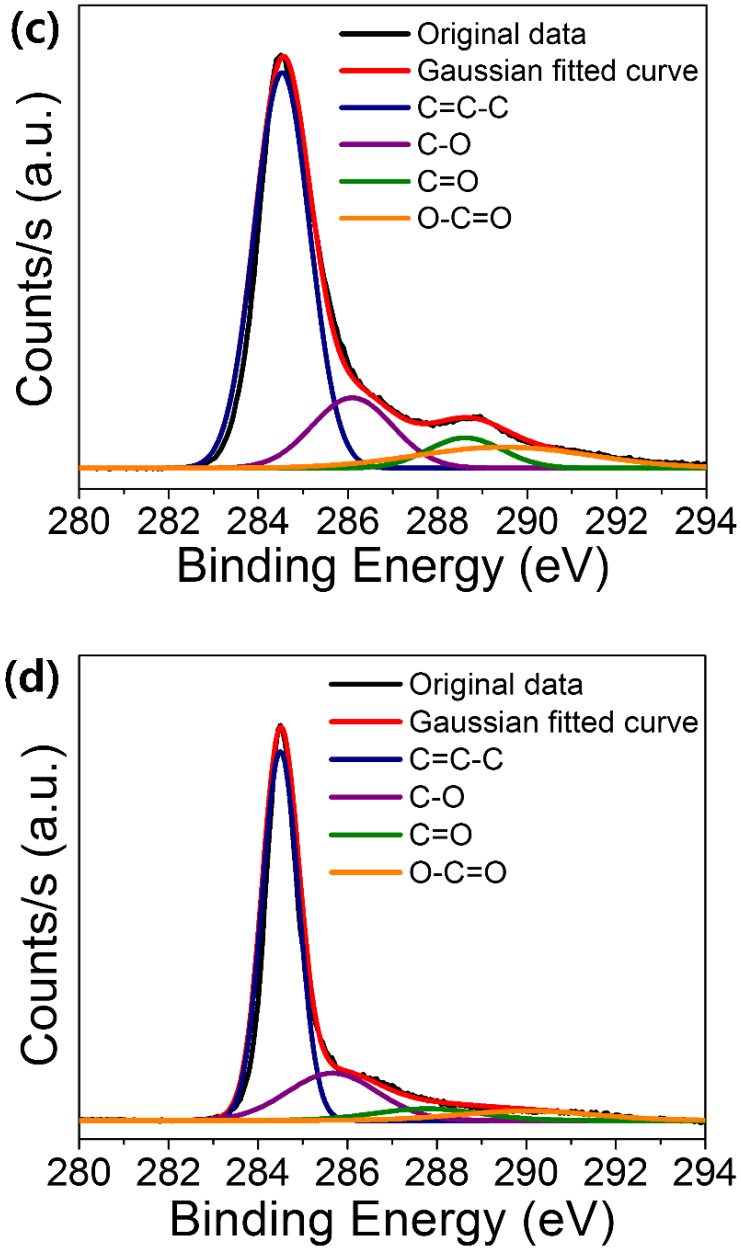

Figure 13. (a) XPS spectra of survey scan and the deconvoluted graphs of C1s peak: (b) CB, (c) a-CB, and (d) EG.

3.2. Tribological property of the nanocomposites

3.2.1 Dispersion state of carbon fillers in TPE matrix

Cryogenically fractured surface of neat TPE and each composites was observed by SEM in order to evaluate the dispersion state of the carbon fillers in the polymer matrix (Figure 14). The morphology of neat TPE shows quite flat and smooth fractured surface, indicating a typical brittle failure (in the neat crystalline polymer) (Figure 14. (a)) [50]. However, in the CB-TPE composite using untreated carbon black, the fracture surface becomes lumpy due to a formation of carbon black agglomerates (Figure 14. (b)). Large clusters of carbon black aggregates with different shape and size are observed, suggesting poor interaction between carbon black and the polymer matrix [51]. In previous study, a similar phenomenon has also been reported in silica-NBR composites without any surface modifier [52]. On the other hand, surface treated carbon black is dispersed uniformly in the polymer matrix with drastic reduction in size of agglomerates (Figure 14. (c)). This is attribute to the surface modification of carbon black, which increases the interfacial affinity between TPE and the filler, by adopting functional groups on the surface of carbon black. This result is consistent with the expectation from the aforementioned results.

Meanwhile, in EG-TPE composites, agglomerates of graphite sheets are not obviously observed, indicating the sheets are well-dispersed (Figure 14. (d)). In addition, the filler embedded in the polymer matrix maintains its 2-dimensional crumpled shape without damage, although it went through a melt mixing process. Lahiri, D. et al. reported that such rumpled graphene sheets greatly improve the mechanical properties of composites due to their high flexibility, as they are easily deformed when force is applied [53]. It can be inferred that the EG has strong interfacial affinity with TPE because the graphite sheets are not pulled out or dropped from the polymer matrix after the fracture [54]. Li, M. &

Jeong, Y. G. conducted a study on EG-PET composites, using thermally exfoliated graphite with few functional groups. Agglomerates of graphite sheets were found in their composites at 1wt% loading [50], whereas, in this work, no agglomerates were found in the EG composite at the same loading. This improved dispersibility of the composite was attribute to the fact that EG was prepared by electrochemical exfoliation method, which is capable of not only manufacturing but also adopting functional groups at the same time. Various hydrophilic functional groups such as carboxyl, hydroxyl and phenolic groups contribute to uniform dispersion of the filler in the polymer matrix and eventually lead an enhancement of the composites' tribological properties.

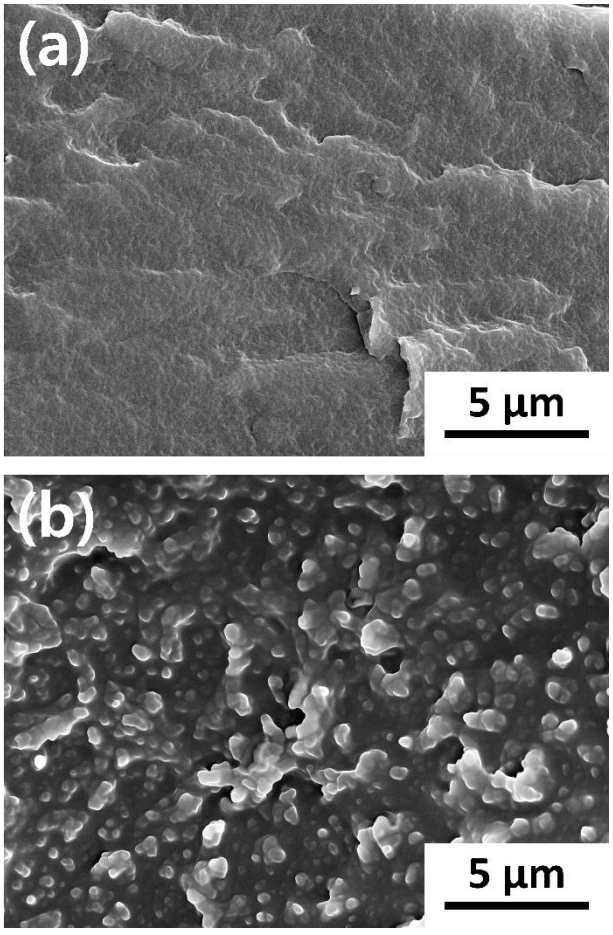

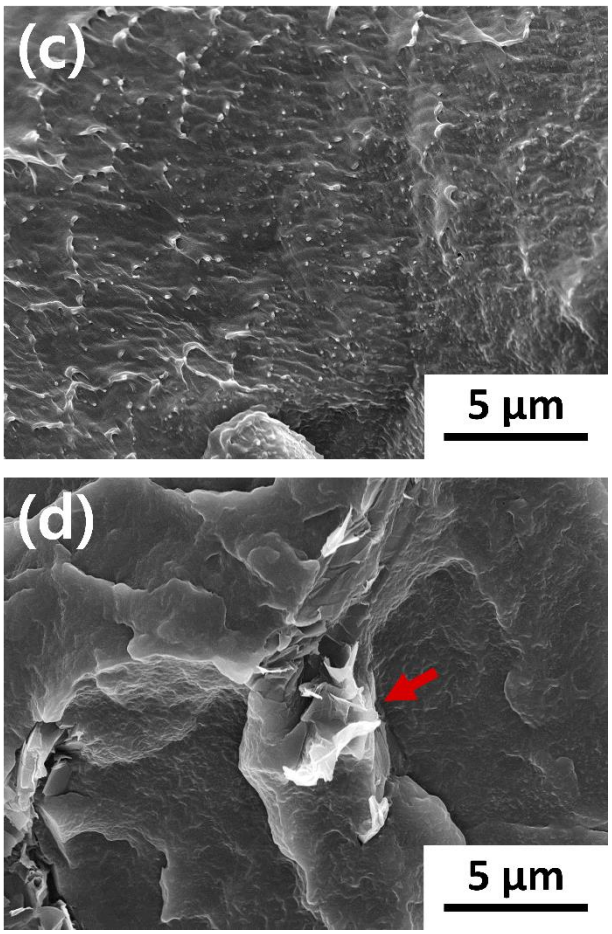

Figure 14. SEM images of fracture surface of (a) neat TPE, (b) CB-TPE, (c) a-CB-TPE, and (d) EG-TPE.

3.2.2 Abrasion test of nanocomposites

An abrasion test was conducted in order to investigate the effect of carbon fillers which have different dimensional structures, on the tribological properties (Figure 15). Weight loss of the neat TPE and the composites was obtained by measuring the weight of specimens before and after the test. The average mass loss of the neat TPE, CB-TPE, a-CB-TPE, and EG-TPE were about 25.1, 16.4, 6.2, 2.3 mg, respectively.

Generally, at low filler content, the tribological properties of the material are strongly dependent on the homogeneity of the dispersion of the nano-fillers in the polymer matrix [55]. Therefore, a-CB, which is expected to be dispersed more uniformly in TPE, exhibits lower weight loss than CB-TPE. In addition, EG-TPE exhibits the lowest weight loss, approximately 11 times lower than neat TPE. Previous studies have investigated the wear rates of multi-layer graphene (MLG) and PVC composites, which were reduced by 56% at 1.2 wt% loading, compared to neat PVC [53]. It is known that graphene which has few layers can greatly increase the wear resistance of the composite, when added to a matrix as a solid lubricant. In the same way, EG shows low friction characteristics due to the layered structure of molecules with weak interlayer bonding that give low shear resistance between atomic layers [56].

When the abrasion occurs between the nanocomposites and the abrasive wheel, the composites were removed from the track forming a wear debris. It generates a lubricating film on the worn surface of the composite due to the low shear resistance of the EG contained in the debris. This lubricating film contributes to protecting the composite surface from wear condition, improving tribological properties.

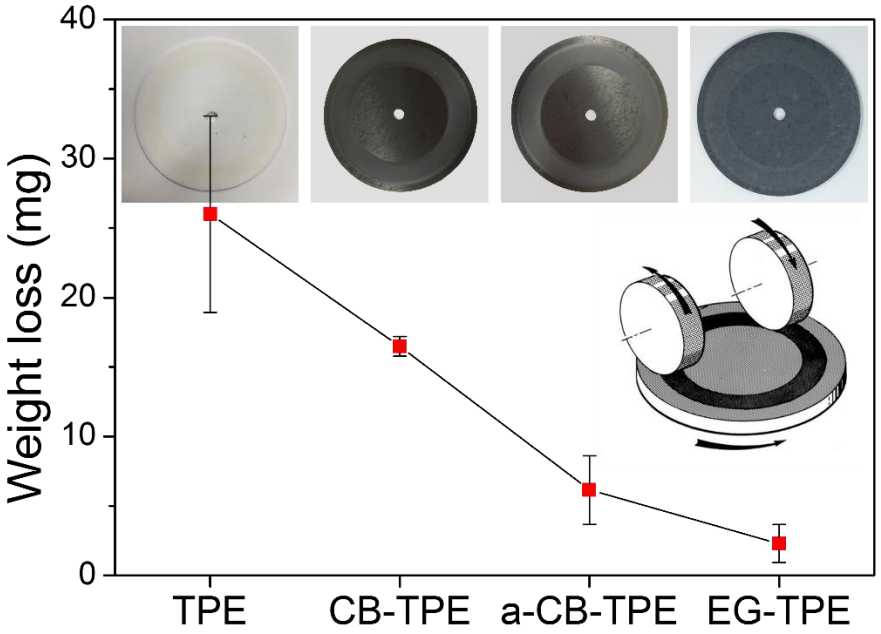

Figure 15. Weight loss of neat TPE and nanocomposites filled with CB, a-CB, EG.

3.2.3 Morphology investigation

3.2.3.1 SEM

Worn surfaces of the nanocomposites after the abrasion test, were investigated by SEM (Figure 16). From the SEM images, it can be seen that the addition of carbon fillers caused changes on morphology of worn surfaces. Neat TPE exhibits the roughest worn surface among the four materials. In addition to, large chunks wear debris is found on the surface, due to its poor wear resistance (Figure 16. (a), (b)). When abrasion occurs, cracks occur at the weak points of materials, and the wear debris broke off from the surface by the adhesive force [57]. Also, deep scratches due to severe adhesion wear and plastic deformation are observed on worn surface. After the CB and a-CB were added to TPE, the worn surface of the composites becomes smoother compared to the neat TPE. Moreover, the size and amount of wear debris has been decreased (Figure 16. (c), (d), (e), and (f)). In the case of the EG-TPE composites, worn surfaces that are significantly different from other materials are observed. The scratches on the worn surface, become shallow and fine, and the size of wear debris is very tiny, which is rarely found (Figure 16. (g), (f)). These results indicated that the EG is able to make a lubricant film with low shear strength, on the surface of nanocomposites because of the self-lubricating effect. The lubricant film of the EG can prevent the material from being damaged by forming a crack due to abrasion [58,59].

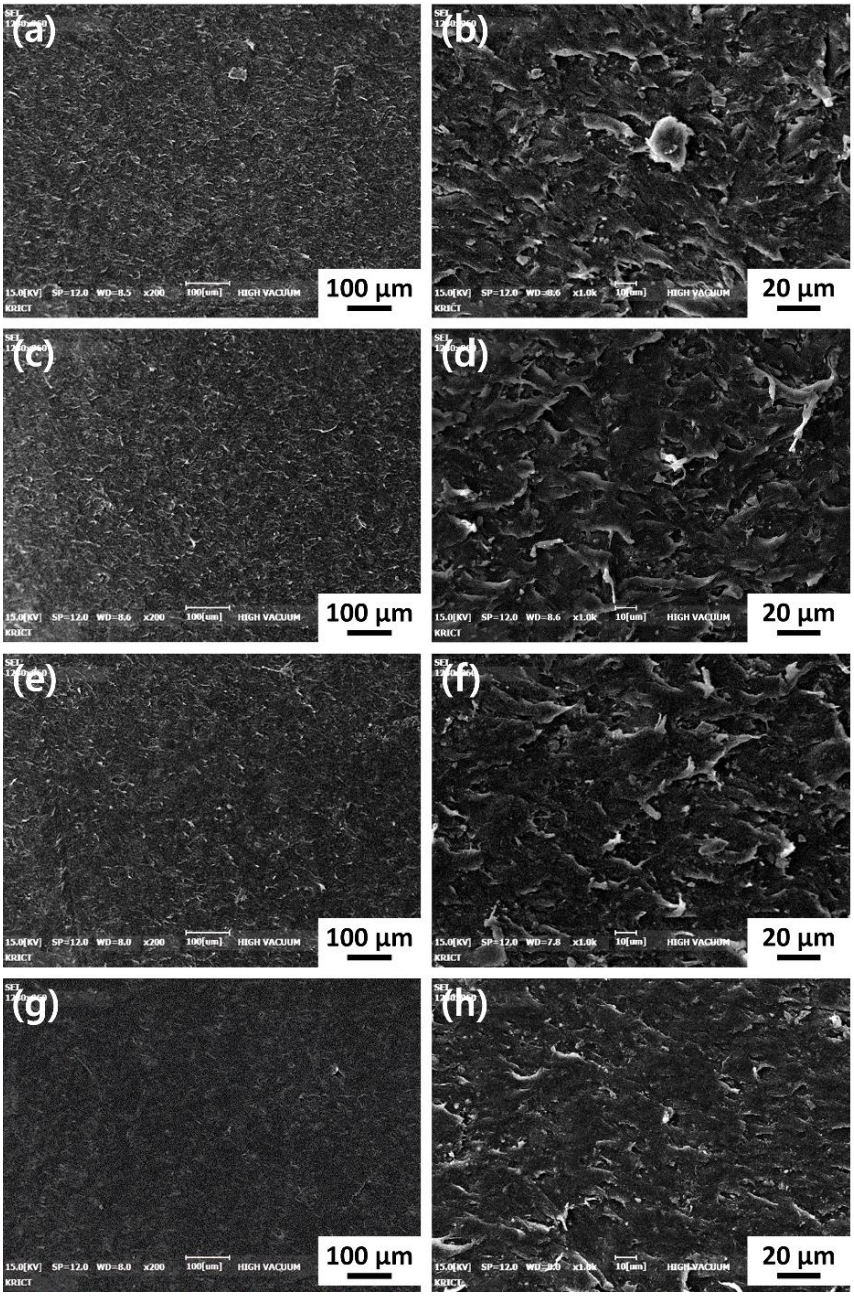

Figure 16. SEM images of worn surface of nanocomposites: (a), (b) neat TPE, (c), (d) CB-TPE, (e), (f) a-CB-TPE, and (g), (h) EG-TPE.

3.2.3.2 Alpha step

Worn surfaces of the nanocomposites after the abrasion test, were observed by Alpha step. The 3D profile images of worn surfaces and the root mean square (RMS) roughness (Figure 17). In 3D profile images, it can be deduced that the worn surface gradually becomes smooth in order of neat TPE, CB-TPE, a-CB-TPE, and EG-TPE (Figure 17. (a), (b), (c), and (d)). These results exhibit the same tendency with the result of SEM images. The RMS roughness of the nanocomposites decreases steadily in the same order (Figure 17. (e)). The RMS roughness of EG was measured at 0.436 nm, which is about 20% lower than that of neat TPE with roughness of 0.566 nm. From the result of worn surface 3D profiling analyses and RMS roughness, it was confirmed that EG has the effect of improving the tribological properties of elastomer, due to its self-lubricating performance.

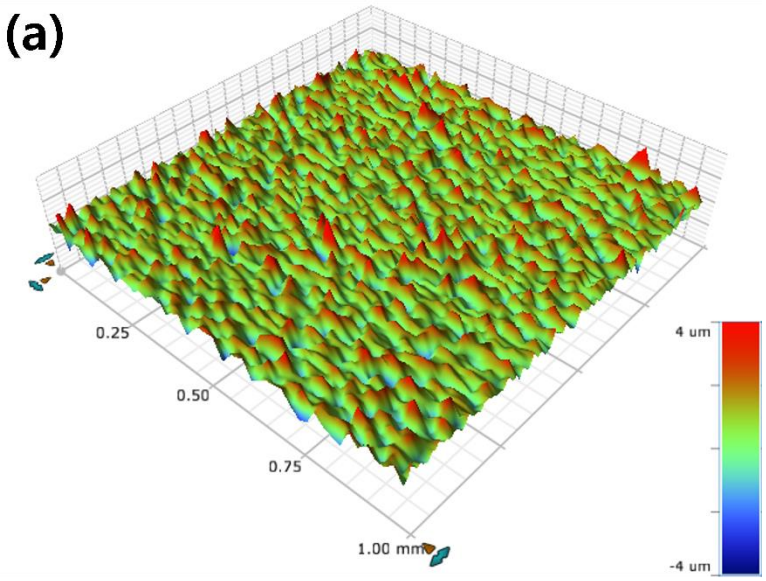

(b)

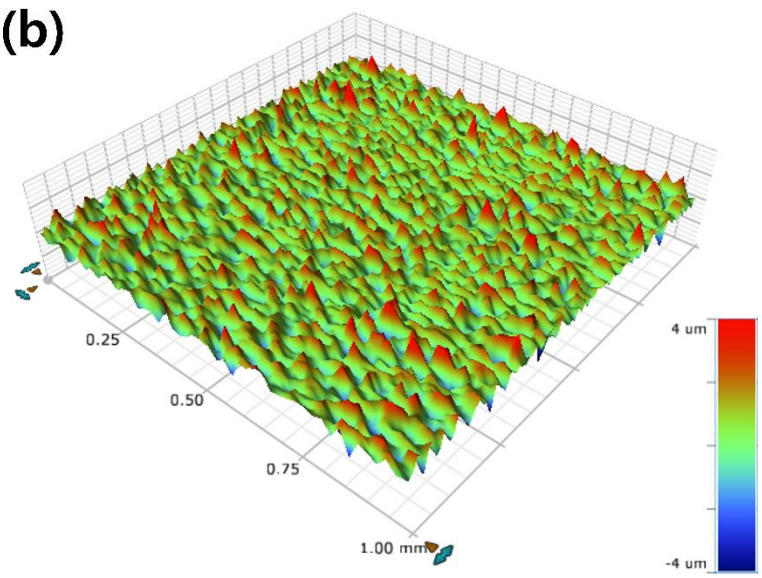

(c)

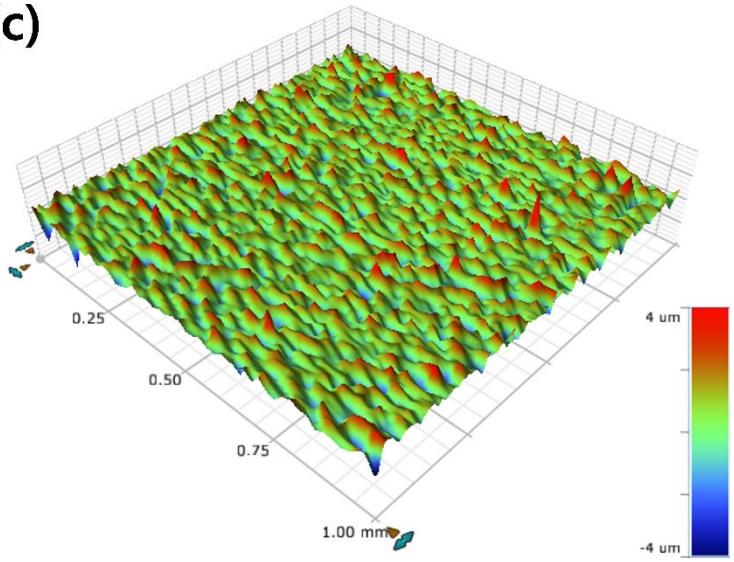

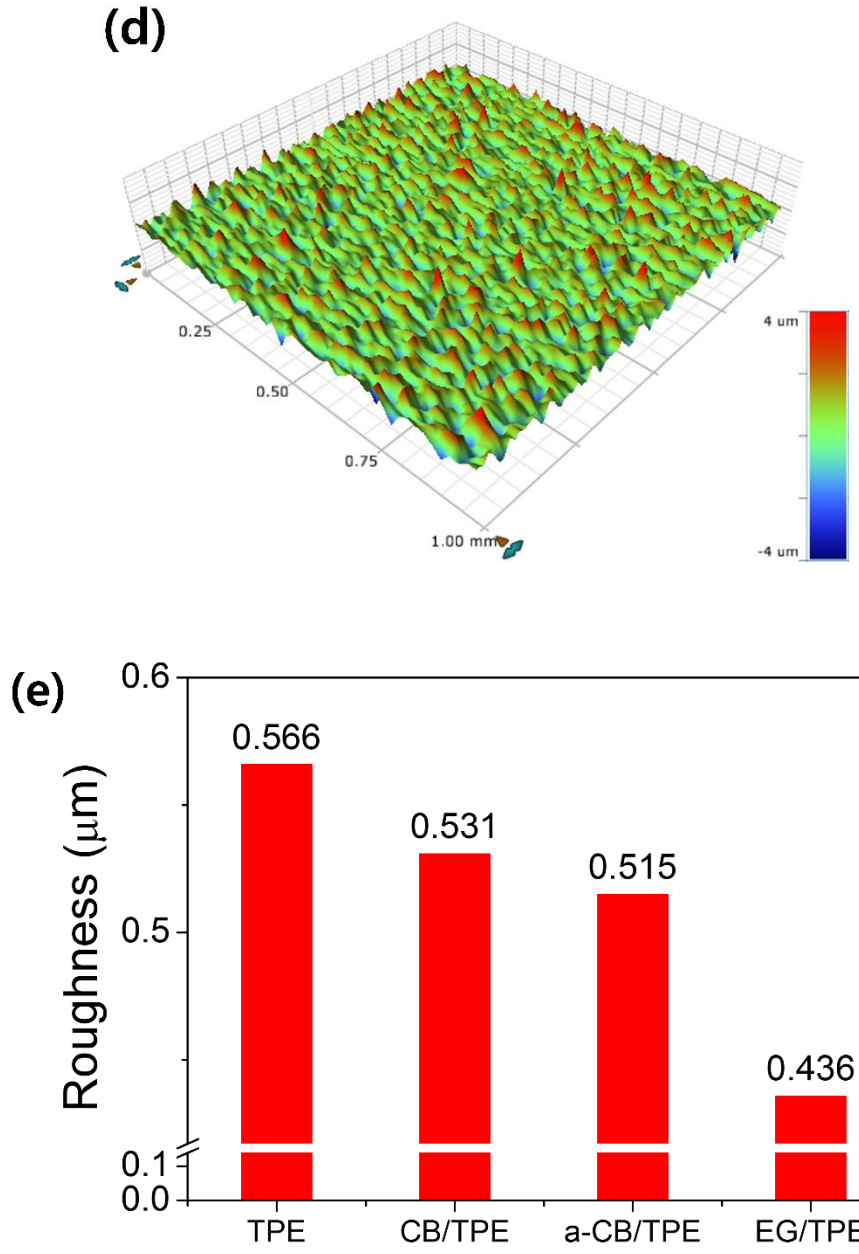

Figure 17. Surface 3D profile images of worn surface of composites: (a) neat TPE, (b) CB-TPE, (c) a-CB-TPE, (d) EG-TPE, and (e) the root mean square (RMS) roughness.

4. Conclusion

In this study, the nanocomposite was prepared with improved abrasion resistance by using electrochemically exfoliated graphite (EG) as a reinforcement filler for elastomer. Compared to neat polymer and nanocomposites filled with carbon black (CB) and surface treated carbon black (a-CB), EG composites exhibit an obvious advantage in enhancing the tribological performance of nanocomposites. In other words, incorporation of EG into an elastomer matrix has led to remarkably improvement of tribological properties. There are several reasons for the benefits of EG sheets. EG has a crumpled sheet structure like graphene with high aspect ratio. In addition, hydrophilic groups including oxygen were adopted on the surface during manufacturing process of EG. For these reasons, it is possible to have better interfacial affinity with elastomers than carbon black. Furthermore, EG has self-lubricating property due to its low shear strength, which is able to make a lubricant film that can prevent the material from being damaged by abrasion.

Reference

1 Myshkin, N., Petrokovets, M. & Kovalev, A. Tribology of polymers: adhesion, friction, wear, and mass-transfer. *Tribology International* **38**, 910-921 (2005).

2 Holmberg, K. & Erdemir, A. Influence of tribology on global energy consumption, costs and emissions. *Friction* **5**, 263-284 (2017).

3 Hutchings, I. Mechanisms of wear in powder technology: a review. *Powder Technology* **76**, 3-13 (1993).

4 Misra, A. & Finnie, I. A classification of three-body abrasive wear and design of a new tester. *Wear* **60**, 111-121 (1980).

5 Dodiya, V. K., Parmar, J., Dodiya, V. K. & Parmar, J. A Study of Various Wear Mechanism and Its Reduction Method. *International Journal* **2**, 242-248.

6 Neale, M. & Gee, M. *A guide to wear problems and testing for industry*. (William Andrew, 2001).

7 Burwell Jr, J. T. Survey of possible wear mechanisms. *Wear* **1**, 119-141 (1957).

8 Harsha, A. & Tewari, U. Two-body and three-body abrasive wear behaviour of polyaryletherketone composites. *Polymer testing* **22**, 403-418 (2003).

9 Dong, H. & Bell, T. State-of-the-art overview: ion beam surface

modification of polymers towards improving tribological properties. *Surface and Coatings Technology* **111**, 29-40 (1999).

10 Nalwa, H. S. *Handbook of organic-inorganic hybrid materials and nanocomposites*. (American Scientific Publishers, 2003).

11 Rong, M., Zhang, M. & Ruan, W. Surface modification of nanoscale fillers for improving properties of polymer nanocomposites: a review. *Materials science and technology* **22**, 787-796 (2006).

12 Quist, A. P., Pavlovic, E. & Oscarsson, S. Recent advances in microcontact printing. *Analytical and bioanalytical chemistry* **381**, 591-600 (2005).

13 LeMieux, M., Peleshanko, S., Anderson, K. & Tsukruk, V. Adaptive nanomechanical response of stratified polymer brush structures. *Langmuir* **23**, 265-273 (2007).

14 Mirfakhrai, T., Madden, J. D. & Baughman, R. H. Polymer artificial muscles. *Materials today* **10**, 30-38 (2007).

15 Abgrall, P. & Nguyen, N. T. Nanofluidic devices and their applications. *Analytical chemistry* **80**, 2326-2341 (2008).

16 Brosseau, C., NDong, W. & Mdarhri, A. Influence of uniaxial tension on the microwave absorption properties of filled polymers. *Journal of Applied Physics* **104**, 074907 (2008).

17 Likozar, B. & Major, Z. Morphology, mechanical, cross-linking, thermal, and tribological properties of nitrile and hydrogenated nitrile rubber/multi-walled carbon nanotubes composites prepared by melt

compounding: The effect of acrylonitrile content and hydrogenation. *Applied Surface Science* **257**, 565-573 (2010).

18 Spahr, M. E. & Rothon, R. Carbon black as a polymer filler. *Fillers for Polymer Applications*, 261-291 (2017).

19 Schaefer, D. *et al*. Multilevel structure of reinforcing silica and carbon. *Journal of Applied Crystallography* **33**, 587-591 (2000).

20 Schaefer, D. W., Suryawanshi, C., Pakdel, P., Ilavsky, J. & Jemian, P. R. Challenges and opportunities in complex materials: silica-reinforced elastomers. *Physica A: Statistical Mechanics and its Applications* **314**, 686-695 (2002).

21 Koga, T., Takenaka, M., Aizawa, K., Nakamura, M. & Hashimoto, T. Structure factors of dispersible units of carbon black filler in rubbers. *Langmuir* **21**, 11409-11413 (2005).

22 Rieker, T. P., Hindermann-Bischoff, M. & Ehrburger-Dolle, F. Small-angle X-ray scattering study of the morphology of carbon black mass fractal aggregates in polymeric composites. *Langmuir* **16**, 5588-5592 (2000).

23 Donnet, J.-B. *Carbon black: science and technology*. (CRC Press, 1993).

24 Cai, M., Thorpe, D., Adamson, D. H. & Schniepp, H. C. Methods of graphite exfoliation. *Journal of Materials Chemistry* **22**, 24992-25002 (2012).

25 Novoselov, K. S. *et al.* Electric field effect in atomically thin carbon

films. *science* **306**, 666-669 (2004).

26 Liu, F., Ming, P. & Li, J. Ab initio calculation of ideal strength and phonon instability of graphene under tension. *Physical Review B* **76**, 064120 (2007).

27 Yan, Q. *et al.* Intrinsic current− voltage characteristics of graphene nanoribbon transistors and effect of edge doping. *Nano letters* **7**, 1469-1473 (2007).

28 Lee, J.-U., Yoon, D., Kim, H., Lee, S. W. & Cheong, H. Thermal conductivity of suspended pristine graphene measured by Raman spectroscopy. *Physical Review B* **83**, 081419 (2011).

29 Novoselov, K. S. *et al.* A roadmap for graphene. *nature* **490**, 192 (2012).

30 Stoller, M. D., Park, S., Zhu, Y., An, J. & Ruoff, R. S. Graphene-based ultracapacitors. *Nano letters* **8**, 3498-3502 (2008).

31 Yi, M. & Shen, Z. A review on mechanical exfoliation for the scalable production of graphene. *Journal of Materials Chemistry A* **3**, 11700-11715 (2015).

32 Stankovich, S. *et al.* Stable aqueous dispersions of graphitic nanoplatelets via the reduction of exfoliated graphite oxide in the presence of poly (sodium 4-styrenesulfonate). *Journal of Materials Chemistry* **16**, 155-158 (2006).

33 Israelachvili, J. N. *Intermolecular and surface forces*. (Academic press, 2011).

34 Ang, P. K., Wang, S., Bao, Q., Thong, J. T. & Loh, K. P. High-throughput synthesis of graphene by intercalation− exfoliation of graphite oxide and study of ionic screening in graphene transistor. *Acs Nano* **3**, 3587-3594 (2009).

35 Coleman, J. N. Liquid-phase exfoliation of nanotubes and graphene. *Advanced Functional Materials* **19**, 3680-3695 (2009).

36 Oyer, A. J. *et al.* Stabilization of graphene sheets by a structured benzene/hexafluorobenzene mixed solvent. *Journal of the American Chemical Society* **134**, 5018-5021 (2012).

37 Parvez, K. *et al.* Exfoliation of graphite into graphene in aqueous solutions of inorganic salts. *Journal of the American Chemical Society* **136**, 6083-6091 (2014).

38 Chung, D. A review of exfoliated graphite. *Journal of materials science* **51**, 554-568 (2016).

39 Novoselov, K. *et al.* Two-dimensional atomic crystals. *Proceedings of the National Academy of Sciences* **102**, 10451-10453 (2005).

40 Parvez, K. *et al.* Electrochemically exfoliated graphene as solution-processable, highly conductive electrodes for organic electronics. *ACS nano* **7**, 3598-3606 (2013).

41 Liu, N. *et al.* One-step ionic-liquid-assisted electrochemical synthesis of ionic-liquid-functionalized graphene sheets directly from graphite. *Advanced Functional Materials* **18**, 1518-1525 (2008).

42 Lee, J. H. *et al.* One-step exfoliation synthesis of easily soluble graphite

and transparent conducting graphene sheets. *Advanced Materials* **21**, 4383-4387 (2009).

43 Yu, P., Lowe, S. E., Simon, G. P. & Zhong, Y. L. Electrochemical exfoliation of graphite and production of functional graphene. *Current Opinion in Colloid & Interface Science* **20**, 329-338 (2015).

44 Su, C.-Y. *et al.* High-quality thin graphene films from fast electrochemical exfoliation. *ACS nano* **5**, 2332-2339 (2011).

45 Yuan, J., Hong, R., Wang, Y. & Feng, W. Low-temperature plasma preparation and application of carbon black nanoparticles. *Chemical Engineering Journal* **253**, 107-120 (2014).

46 Zappielo, C. D. *et al.* Solid phase extraction to on-line preconcentrate trace cadmium using chemically modified nano-carbon black with 3-mercaptopropyltrimethoxysilane. *Journal of the Brazilian Chemical Society* **27**, 1715-1726 (2016).

47 Lyth, S. *et al.* Solvothermal synthesis of superhydrophobic hollow carbon nanoparticles from a fluorinated alcohol. *Nanoscale* **7**, 16087-16093 (2015).

48 Li, X. *et al.* Large-area synthesis of high-quality and uniform graphene films on copper foils. *science* **324**, 1312-1314 (2009).

49 Peng, C., Lang, J., Xu, S. & Wang, X. Oxygen-enriched activated carbons from pomelo peel in high energy density supercapacitors. *RSC Advances* **4**, 54662-54667 (2014).

50 Li, M. & Jeong, Y. G. Poly (ethylene terephthalate)/exfoliated graphite

nanocomposites with improved thermal stability, mechanical and electrical properties. *Composites Part A: Applied Science and Manufacturing* **42**, 560-566 (2011).

51 Al-Hartomy, O. A. *et al.* Influence of carbon black/silica ratio on the physical and mechanical properties of composites based on epoxidized natural rubber. *Journal of Composite Materials* **50**, 377-386 (2016).

52 Kapgate, B. P., Das, C., Basu, D., Das, A. & Heinrich, G. Rubber composites based on silane-treated stöber silica and nitrile rubber: Interaction of treated silica with rubber matrix. *Journal of Elastomers & Plastics* **47**, 248-261 (2015).

53 Wang, H., Xie, G., Zhu, Z., Ying, Z. & Zeng, Y. Enhanced tribological performance of the multi-layer graphene filled poly (vinyl chloride) composites. *Composites Part A: Applied Science and Manufacturing* **67**, 268-273 (2014).

54 Lahiri, D. *et al.* Nanotribological behavior of graphene nanoplatelet reinforced ultra high molecular weight polyethylene composites. *Tribology International* **70**, 165-169 (2014).

55 Malucelli, G. & Marino, F. in *Abrasion resistance of materials* (InTech, 2012).

56 Dienwiebel, M. *et al.* Superlubricity of graphite. *Physical review letters* **92**, 126101 (2004).

57 Hongtao, L., Shirong, G., Shoufan, C. & Shibo, W. Comparison of wear debris generated from ultra high molecular weight polyethylene in vivo

and in artificial joint simulator. *Wear* **271**, 647-652 (2011).

58 Ye, J., Khare, H. & Burris, D. Transfer film evolution and its role in promoting ultra-low wear of a PTFE nanocomposite. *Wear* **297**, 1095-1102 (2013).

59 Chang, L., Friedrich, K. & Ye, L. Study on the transfer film layer in sliding contact between polymer composites and steel disks using nanoindentation. *Journal of Tribology* **136**, 021602 (2014).

초 록

재료의 내마모 특성은 재료가 마모에 저항할 수 있는 특성으로, 다양한 산업 분야에서의 활용을 위한 고 내마모성 소재의 개발이 필요한 추세입니다. 종래에는 엘라스토머의 내마모성 보강제로 탄소 소재인 카본블랙을 사용해 왔으며 이의 표면처리 및 분산제에 관한 연구가 활발히 진행되어 왔습니다. 내마모성의 향상을 위해서는 고분자 매트릭스와 충전제 간의 결합력이 중요하며, 이는 충전제의 표면 특성 및 구조 형태에 따라 결정됩니다. 충전제에 표면 처리를 하거나 구조가 발달한 소재를 사용할 경우 고분자와 충전제 간 결합력이 개선되어 높은 내마모 특성을 구현할 수 있습니다. 이처럼 카본블랙의 표면처리를 통해 고분자 내 분산성을 어느 정도 개선할 수 있으나, 구조적인 측면에서 한계점이 있으므로, 새로운 탄소 충전제의 개발이 필요한 실정입니다.

본 연구에서는 박리흑연과 카본블랙을 사용하여 나노복합재를 제조하고, 각 복합재의 마모 감량을 측정하고 비교하였습니다. 복합재의 충전제로써 그래핀과 유사한 특성을 갖는 박리흑연을 전기화학적 방식으로 제조하여 사용하였습니다. 또한, 카본블랙과, 고분자 내 분산성을 개선시키기 위하여 표면 처리를 진행한 카본블랙을 제조하였습니다. 이렇게 준비한 세가지 탄소 충전제와 열가소성 엘라스토머를 연속식 압출 공정을 통해 컴파운딩하여

나노복합소재를 제조하였습니다. 각 소재의 마모 시험 전 후의 무게 차이를 측정하여 마모 감량을 계산하고 비교하였습니다. 그 결과, 박리흑연 복합재는 엘라스토머 단독 소재 대비 91% 감소한 마모 감량을 보였으며, 카본블랙 및 표면 처리된 카본블랙 복합재보다 뚜렷한 우수한 마모 저항성을 보였습니다. 박리흑연 복합재의 우수한 내마모 특성은 아래의 이유로 설명될 수 있습니다. 먼저, 박리흑연의 높은 종횡비와 제조 과정에서 도입된 친수성 관능기들이 엘라스토머와의 계면 결합력을 개선시켰기 때문입니다. 또한, 박리흑연을 구성하고 있는 그래핀 시트의 자기윤활 특성으로 인해 마모 표면에 윤활막이 형성되어, 재료가 마모되는 것을 막아주기 때문입니다. 따라서, 전기화학적 박리흑연 복합재는 기존의 카본블랙 복합재를 대체하여 고 내마모성이 요구되는 분야에 적용하기에 적합할 것으로 예상됩니다.

주요어: 박리흑연, 카본블랙, 열가소성 엘라스토머, 탄소 나노복합소재, 개선된 마모저항 특성

학 번: 2017-24895